VLUGR2:
A Vectorizable Adaptive Grid Solver for PDEs in 2D

J.G. Blom, R.A. Trompert, and J.G. Verwer

CWI

P.O. Box 94079, 1090 GB Amsterdam, The Netherlands

Abstract

This paper deals with an adaptive-grid finite-difference solver for time-dependent two-dimensional systems of partial differential equations. It describes the `ANSI FORTRAN 77` code, `VLUGR2`, auto-vectorizable on the Cray Y-MP, that is based on this method. The robustness and the efficiency of the solver, both for vector and scalar processors, is illustrated by the application of the code to two example problems arising from a groundwater-flow model.

AMS Subject Classification (1991): Primary: 65-04. Secondary: 65M20, 65M50, 65F10, 65Y20.
CR Subject Classification (1991): G.1.8, J.2.
Keywords & Phrases: software, partial differential equations, method of lines, adaptive grid methods, non-symmetric sparse linear systems, iterative solvers, vectorization.
Note: This work was supported by Cray Research, Inc., under grant CRG 92.05, via the Stichting Nationale Computerfaciliteiten (National Computing Facilities Foundation, NCF).

1. Introduction

In previous work [11, 12, 13, 15, 14, 16, 10] an adaptive-grid finite-difference method to solve time-dependent two-dimensional systems of partial differential equations (PDEs) was discussed. Among others, a research code, `MOORKOP`[9], was developed that uses an implicit time-stepping method. In [1] we described a `FORTRAN 77` code, `VLUGR2`, that is based on `MOORKOP` but with the intention to use it on a vector processor. To that aim the datastructure was adapted to facilitate the vector processing of the most time consuming parts of the code, and to make the use of memory as compact and as small as possible.

In this paper we describe the final version of `VLUGR2`. The main difference with the version in [1] is the solution of the systems of nonlinear equations. The nonlinear systems in `VLUGR2` are solved by a choice from three solvers. The first two use modified Newton with as linear solver either BiCGStab[17] + ILU preconditioning or GCRO[8] with a simple (block) diagonal scaling. The third option is a matrix-free implementation of the second solver. Also the implementation of the time integration part slightly differs from [1] and is now identical to the implementation used in `VLUGR3`, which is the 3D extension of `VLUGR2`. The 3D code is described in detail in [3, 4].

The paper is organized as follows. In Section 2 we define the problem class of `VLUGR2`. Section 3 is devoted to an outline of the Local Uniform Grid Refinement method as implemented in `VLUGR2` and contains a survey of the choices made in the code with respect to the refinement strategy and the integration strategy including the solution of the arising (non)linear systems. In Section 4 we discuss the for a user relevant part of the implementation and the amount of data storage required. There we also describe how to use `VLUGR2`, enlightened by an elaborated example problem. In Section 5 we discuss the performance of `VLUGR2` on the same groundwater-flow problems as were used in [14, 1]. The performance evaluations were done on a Cray Y-MP in scalar and vector mode. Finally, Section 6 contains a summary of our findings.

2. PDE definition

VLUGR2 has been designed to solve initial boundary value problems for systems of partial differential equations that fit in the following master equation

$$\mathcal{F}(t, x, y, \mathbf{u}, \mathbf{u}_t, \mathbf{u}_x, \mathbf{u}_y, \mathbf{u}_{xx}, \mathbf{u}_{xy}, \mathbf{u}_{yy}) = 0, \quad (x, y) \in \Omega, \quad t > t_0, \tag{2.1}$$

where the solution $\mathbf{u}$ may be a vector and the domain Ω an arbitrary domain that can be described by right-angled polygons (see, e.g., Fig. 1). The boundary conditions belonging to system (2.1) are formulated as

$$\mathcal{B}(t, x, y, \mathbf{u}, \mathbf{u}_t, \mathbf{u}_x, \mathbf{u}_y) = 0, \quad (x, y) \in \partial\Omega, \quad t > t_0, \tag{2.2}$$

and the initial conditions satisfy

$$\mathbf{u}(t_0, x, y) = \mathbf{u}_0(x, y), \quad (x, y) \in \Omega \cup \partial\Omega. \tag{2.3}$$

3. The algorithm

In this section we give a short survey of the algorithm. We discuss the method parameters of VLUGR2 that can be specified by the user. For further information about algorithmic aspects we refer to [3].

3.1 Outline of the LUGR algorithm

The virtue of a Local Uniform Grid Refinement method lies in the fact that one reaches the accuracy of a fine mesh width with considerably less computational effort and memory requirements, since the fine subgrids cover only part of the domain. The concept of such a method is simple. Starting from a, uniform, coarse base grid covering the whole domain, ever finer uniform subgrids are recursively created in a nested way in regions with high spatial activity. So all grid levels consist of one or more disjunct sets of interconnected grid cells, all having the same size. Each time step a new initial boundary value problem is solved at all grid levels ordered from coarse to fine. The fine grid solution values are injected in the coinciding coarser grid nodes. The location and size of the subgrids are adjusted each time step to follow, e.g., the movement of the steep parts of the solution.

For the space discretization standard second-order finite differences are used, central on the internal domain and one-sided at the boundaries. At 'internal' corners, i.e., with an angle of 270^0, we use also one-sided differencing to prevent difficulties with the ILU decomposition of the Jacobian in the Newton process. Where grid refinement is required we divide a grid cell in 4 equal parts. Where interpolation is needed to get solution values, linear interpolation is used.

The refinement is governed by a curvature monitor. For each grid point (i, j) this monitor is determined by

$$\texttt{SPCMON}(i, j) := \max_{ic=1,\texttt{NPDE}} \texttt{SPCTOL}(ic) \cdot (|\Delta x^2 \cdot u_{xx}^{ic}(i, j)| + |\Delta y^2 \cdot u_{yy}^{ic}(i, j)|), \tag{3.1}$$

where Δx and Δy are the grid width in the x- and the y-direction, respectively, and

$$\texttt{SPCTOL}(ic) := \frac{\texttt{SPCWGT}(ic)}{\texttt{UMAX}(ic) \cdot \texttt{TOLS}}. \tag{3.2}$$

The variables on the right-hand side of (3.2) are user specified quantities, $0 \leq \texttt{SPCWGT} \leq 1$ a weighting factor for the relative importance of a PDE component on the space monitor, UMAX the, approximate, maximum absolute value for each component, and TOLS the space tolerance.

VLUGR2 also offers the possibility to enforce grid refinement in a priori selected regions by adapting the SPCMON values (see Section 4.4).

3.2 Integration in time

We solve the system of PDEs using the Method of Lines approach. The PDEs are discretized in space and the resulting system of ODEs or DAEs is solved in time using the second-order two-step implicit BDF method with variable step sizes. In the first time step we apply as usual Backward Euler. The time integration is controlled by a second solution monitor, viz., the maximum over all existing grid levels of

$$\|\Delta t\, \mathbf{u}_t\|_w, \tag{3.3}$$

where Δt is the current time step size and $\mathbf{u}_t$ is approximated by first-order finite differences. The norm used in (3.3) is a weighted root-mean-square norm

$$\|\mathbf{v}\|_w = \|W\mathbf{v}\|_2, \tag{3.4}$$

with W a diagonal matrix given by

$$W = 1/\sqrt{N}\; diag(w_1, ..., w_N). \tag{3.5}$$

The entries w_i of the diagonal matrix W are defined by

$$w_{ipt,ic} = \texttt{TIMWGT}(ic)/(\texttt{ABSTOL}(ic) + |U^{n+1}_{ipt,ic}| \cdot \texttt{RELTOL}(ic)), \quad ipt \in \Omega \text{ and } ic = 1, \texttt{NPDE}, \tag{3.6}$$

with

$$\texttt{ABSTOL}(ic) = 0.01 \cdot \texttt{TOLT} \cdot \texttt{UMAX}(ic) \text{ and } \texttt{RELTOL}(ic) = \texttt{TOLT}. \tag{3.7}$$

The variables TIMWGT and TOLT are the, user specified, analogues of the variables in (3.2).

To solve the resulting system of nonlinear equations a Newton process is used combined with a preconditioned iterative linear solver. The stopping criterion for the Newton process is

$$\frac{\rho}{1-\rho}\|\mathbf{U}^{(k)} - \mathbf{U}^{(k-1)}\|_w < \texttt{TOLNEW}, \tag{3.8}$$

where ρ is an approximation of the convergence rate. The entries w_i of the diagonal matrix W in (3.4)-(3.5) are here defined by

$$w_{ipt,ic} = 1.0/(\texttt{ATOL}(ic) + |U^{(0)}_{ipt,ic}| \cdot \texttt{RTOL}(ic)), \quad ipt \in \Omega \text{ and } ic = 1, \texttt{NPDE}, \tag{3.9}$$

with

$$\texttt{ATOL}(ic) = 0.01 \cdot \texttt{TOL} \cdot \texttt{UMAX}(ic) \text{ and } \texttt{RTOL}(ic) = \texttt{TOL}; \qquad \texttt{TOL} = 0.1 \min(\texttt{TOLT}^2, \texttt{TOLS}). \tag{3.10}$$

For the linear solver the stopping criterion reads

$$\|P^{-1} r^{(l)}\|_w < \texttt{TOLLSS}/2^k, \tag{3.11}$$

with k the current Newton-iteration index and P^{-1} the preconditioner. Both stopping criteria can be influenced easily by the user by changing the value of TOLNEW (default 1.0) and TOLLSS (TOLNEW/10) in parameter statements. The maximum number of iterations in both solvers can also be set via parameter statements.

In VLUGR2 the nonlinear systems can be solved with modified Newton and the linear systems either with BiCGStab[17] with ILU preconditioning or with GCRO[8] and (block) diagonal scaling as preconditioner. GCRO is a recursive variant of GCR in which the inner (GMRES) loop dynamically generates a preconditioner. A third possibility is to use matrix-free Newton combined with the latter linear solver. In the first two solvers the Jacobian matrix is computed by numerical differencing, once per time step, and stored. How to approximate the entries of the Jacobian is discussed in [1, 3]. For the problems we solved with the code the approximation of the Jacobian was sufficiently accurate.

However, if for a specific problem Newton failures would often be the cause of time step failures, it could be worthwhile to store the exact partial derivatives instead of the approximated ones (see Section 4.4).

For the solvers that make explicit use of the Jacobian we developed in [2] a vectorizable implementation of the matrix-vector multiply and of the ILU preconditioning routines. This implementation is designed especially for systems of PDEs in 2D discretized on a 9-point stencil and on a grid that is bounded by arbitrary right-angled polygons.

In the third solver the product of the Jacobian times a vector, which is the only need for the Jacobian when using GCRO (or BiCGStab), is approximated by a difference quotient on the residual. In this case the vector performance of the matrix-vector multiply is of course determined by the user implementation of the residual evaluation. An advantage of this solver is that it allows an easy change of space-discretization schemes resulting in other couplings than the 9-point stencil.

4. The code

4.1 Datastructure

To achieve a good vector performance, pointers are stored to the boundary points in the grid structure so that, e.g., the computation of the PDE can be performed in two 'sweeps'. In the first, using direct addressing, the PDE residual on the internal domain (2.1) is computed over the whole domain, including the boundary. In the second sweep, using indirect addressing, the values on the boundary are reset by incorporating the boundary conditions (2.2).

The solution at a specific grid level is stored row-wise, one component vector after the other. Solutions from 3 different time levels are saved. For the oldest time level only the injected solution values for the computation of $\mathbf{U}_t$ with the BDF method. For the previous time level also the original, not-injected, solution is needed to serve as an initial solution estimate in the Newton process.

A grid at a specific grid level is stored in the following datastructure

- `LROW`: the actual number of rows in the grid, the pointers to the start of a row in the grid, and the number of grid points
- `IROW`: the row number of a row in the (virtual) rectangle
- `ICOL`: the column number of a grid point in the (virtual) rectangle
- `LLBND`: the total number of physical boundaries and corners in the actual domain, the pointers to the start of a specific boundary or corner in `LBND`, and the number of boundary points
- `ILBND`: the type of the boundaries

  1: lower boundary
  2: left boundary
  3: upper boundary
  4: right boundary
  12: lower left corner (90^0)
  23: left upper corner (90^0)
  34: upper right corner (90^0)
  41: right lower corner (90^0)
  21: left lower corner (270^0)
  32: upper left corner (270^0)
  43: right upper corner (270^0)

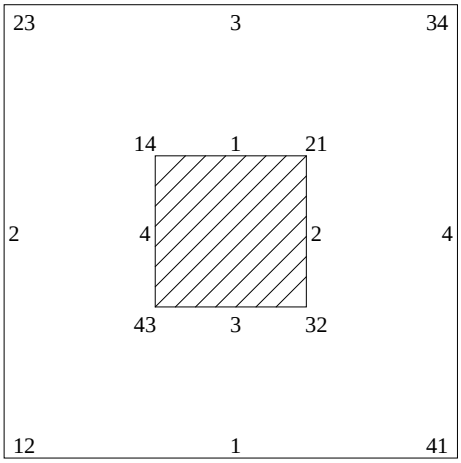

14: lower right corner (270^0)

- LBND: the pointers to the boundary points in the actual grid
- LBELOW: pointer to node below in the actual grid or 0, if index node is lower boundary point
- LABOVE: pointer to node above in the actual grid or 0, if index node is upper boundary point.

All grids from the three different time levels are saved. For the base grid all information is saved, i.e., the arrays containing the grid information, the pointer arrays needed for the Jacobian and the pointer arrays for the hyperplane ordering. The latter is done even if the matrix-free option is chosen, to facilitate a continuation of the integration using another solver. For the higher level grids only the first 3 arrays (LROW,IROW,ICOL) are saved.

The above mentioned arrays and workspace for the nonlinear system solver are stored consecutively in the real and integer work arrays. Pointers for each time and grid level indicate the start in a work array of a solution or grid at a specific time and at a specific grid level. For a more complete description of the contents of the work arrays we refer to the documentation of the enveloping routine VLUGR2.

4.2 Data storage requirements

Many architectures have a relatively small main memory and make use of so-called virtual memory. On those systems the real-time performance is often not determined by the floating-point operations but by memory operations (data swap). Therefore our goal was to keep the amount of workspace small, and to store all data in a compact way.

VLUGR2 requires roughly the following amount of memory

$$\texttt{INTEGER}: \quad 5 \cdot \texttt{MAXLEV} \cdot \texttt{NPTS}_{av} + 5 \cdot \texttt{NPTS}_{max} + \texttt{LSSIWK}$$

$$\texttt{REAL}: \quad 5 \cdot \texttt{MAXLEV} \cdot \texttt{NPDE} \cdot \texttt{NPTS}_{av} + (2 + 9 \cdot \texttt{NPDE}) \cdot \texttt{NPTS}_{max} + \texttt{LSSRWK}$$

where $\texttt{NPTS}_{av}$ is the average number of grid points over all grid levels and $\texttt{NPTS}_{max}$ is the maximum number of grid points on any level. The workstorage needed for the linear system solver (including Jacobian and/or preconditioner) is when using BiCGStab + ILU

$$\texttt{LSSIWK}: \quad 9 \cdot \texttt{NPTS}_{max}$$

$$\texttt{LSSRWK}: \quad 18 \cdot \texttt{NPDE} \cdot \texttt{NPTS}_{max} \cdot \texttt{NPDE}.$$

When using GCRO with the Jacobian approximated and stored

$$\texttt{LSSIWK}: \quad 6 \cdot \texttt{NPTS}_{max}$$

and the real workspace is dependent on the choice of the preconditioner:
GCRO + block-diagonal scaling

$$\texttt{LSSRWK}: \quad \texttt{JACRWK} + \texttt{NPTS}_{max} \cdot \texttt{NPDE} \cdot (\max(\texttt{NPDE} \cdot 5 + 3, 2 \cdot \texttt{MAXLR} + \texttt{MAXL} + 5) + \texttt{NPDE}),$$

GCRO + diagonal scaling

$$\texttt{LSSRWK}: \quad \texttt{JACRWK} + \texttt{NPTS}_{max} \cdot \texttt{NPDE} \cdot (2 \cdot \texttt{MAXLR} + \texttt{MAXL} + 6),$$

with $\texttt{JACRWK} = 9 \cdot \texttt{NPDE} \cdot \texttt{NPTS}_{max} \cdot \texttt{NPDE}$. When using matrix-free GCRO, $\texttt{LSSIWK} = 0$ and the real workspace is as before with $\texttt{JACRWK} = 0$. In the above MAXLR is the maximum number of outer GCR iterations and MAXL is the maximum number of inner GMRES iterations. These values can be adapted via parameter statements.

The workstorage required will be checked against the user defined workspace. If the workspace is too small, a message is printed with the needed amount given.

4.3 How to use VLUGR2

Our aim was to keep the use of VLUGR2 as simple as possible. Most method parameters are set in parameter statements in the code itself. The user has to specify only the problem parameters and routines. If one wishes to change one of the method parameters the corresponding parameter statements can be changed in the code.

In the simplest case, a well-scaled problem on a rectangle, one has to specify

- the number of PDEs,
- the initial and final time, and the initial step size,
- the lower-left and the upper-right corner of the domain, and the initial grid width in the x- and y-direction,
- the space and time tolerance TOLS and TOLT, and
- the subroutines PDEIV, PDEF, and PDEBC, to specify respectively, the initial solution (2.3), the PDE system at the internal domain (2.1) and the boundary conditions (2.2).

In this case the parameters SPCWGT, TIMWGT and UMAX (cf. (3.2) and (3.6)) are set to their default value, which is 1.

If the initial domain is not a true rectangle, a virtual rectangle is to be placed around the irregular domain. In this case the user should also provide a routine that defines the initial grid. Furthermore, one can supply a routine to enforce grid refinement and a monitor routine for user purposes that will be called after each successful time step (cf. Section 4.4).

4.4 General description

The calling sequence of VLUGR2 is

```
      CALL  VLUGR2 (NPDE, T, TOUT, DT, XL, YL, XR, YU, DX, DY,
     +   TOLS, TOLT, INFO, RINFO, RWK, LENRWK, IWK, LENIWK, LWK, LENLWK,
     +   MNTR)
```

where in the simplest case, using all default values the meaning of the parameters is

NPDE: the number of PDE components

T: the initial time

TOUT: the final time

DT: the initial time step size

(XL,YL): coordinate of lower-left corner of domain (a rectangle)

(XR,YU): coordinate of upper-right corner of domain

DX: cell width in x-direction of base grid

DY: cell width in y-direction of base grid

TOLS: space tolerance

TOLT: time tolerance

INFO: INFO(1) $= 0$, which implies that default parameters are used

RINFO: dummy array

RWK(LENRWK): real workspace, LENRWK $\approx (19+18 \cdot$ NPDE$) \cdot$ NPTS$\cdot$NPDE, with NPTS the expected maximum number of points on a grid

IWK(LENIWK): integer workspace, LENIWK $\approx 24 \cdot$ NPTS

LWK(LENLWK): logical workspace, LENLWK $\approx 2 \cdot$ NPTS

MNTR: MNTR $= 0$, first call of VLUGR2 for this problem.

Furthermore one should supply the routines

PDEIV to specify the initial solution (2.3),

PDEF to specify the PDE system at the internal domain (2.1), and

PDEBC to specify the boundary conditions (2.2).

If one wants to continue the integration after returning from VLUGR2, one should set MNTR to 1. All parameters can be changed although T, DT, XL, YL, XR, YU, DX, and DY will be overwritten with their old values. The contents of the work arrays RWK and IWK should not be altered.

A more sophisticated use can be made with the aid of the INFO and RINFO arrays and by overloading some subroutines. If INFO(1) $\neq 0$ a number of parameters can be specified in INFO and RINFO. The value between brackets is the default value used when INFO(1) $= 0$.

INFO(2): MAXLEV (3), the maximum number of grid levels allowed

INFO(3): RCTDOM (0), if RCTDOM $= 0$ the initial domain is a rectangle, otherwise the user should specify the subroutine INIDOM to define the initial grid (see below)

INFO(4): LINSYS (0), the linear system solver and preconditioner

- **0:** BiCGStab + ILU
- **10:** GCRO + block-diagonal scaling
- **11:** GCRO + block-diagonal scaling (neglecting first-order derivatives at the boundaries)
- **12:** GCRO + diagonal scaling
- **13:** GCRO + diagonal scaling (neglecting first-order derivatives at the boundaries)
- **20:** matrix-free GCRO + block-diagonal scaling
- **21:** matrix-free GCRO + block-diagonal scaling (neglecting first-order derivatives at the boundaries)
- **22:** matrix-free GCRO + diagonal scaling
- **23:** matrix-free GCRO + diagonal scaling (neglecting first-order derivatives at the boundaries)

INFO(5): LUNPDS (0), the logical unit number of the file where information on the integration history will be written. If LUNPDS $= 0$ only global information will be written on standard output

INFO(6): LUNNLS (0), the logical unit number of the file where information on the Newton process will be written. If LUNNLS $= 0$ no information will be written

INFO(7): LUNLSS (0), the logical unit number of the file where information on the linear system solver will be written. If LUNLSS $= 0$ no information will be written

RINFO(1): DTMIN (0.0), the minimum time step size allowed

`RINFO(2)`: `DTMAX` (`TOUT-T`), the maximum time step size allowed

`RINFO(3)`: `UMAX` ((1.0)), the approximate maximum values of the PDE solution components. These values are used for scaling purposes

`RINFO(3+NPDE)`: `SPCWGT` ((1.0)), the weighting factors used in the space monitor to indicate the relative importance of a PDE component on the space monitor

`RINFO(3+2·NPDE)`: `TIMWGT` ((1.0)), the weighting factors used in the time monitor to indicate the relative importance of a PDE component on the time monitor.

The subroutines that are candidates for replacement by the user are

`MONITR` to monitor the solution or the grids; will be called after each successful time step

`CHSPCM` to enforce grid refinement at a specific point in space and time and on a specific level

`INIDOM` to specify the initial grid for a domain that is not rectangular

`DERIVF` to store the exact partial derivatives of the residual $\mathbf{F}$ with respect to (the derivatives of) $\mathbf{U}$.

Finally, the package also contains a number of routines that facilitate the use of the datastructure

`PRDOM` to print the domain one has defined with `INIDOM`

`SETXY` to get the x- and y-coordinates corresponding with the grid points

`PRSOL` to print the solution and the corresponding coordinate values at all grid levels

`DUMP` to dump all necessary information for a restart on file

`RDDUMP` to read all necessary information for a restart from the dump file.

For the details of these routines we refer to the documentation in `VLUGR2`.

4.5 Example problem
Our example problem is the two-dimensional Burgers' system

$$u_t = -uu_x - vu_y + \varepsilon(u_{xx} + u_{yy}) \tag{4.1a}$$

$$v_t = -uv_x - vv_y + \varepsilon(v_{xx} + v_{yy}) \tag{4.1b}$$

on the domain Ω as given in Fig. 1. On the boundaries $\partial\Omega$ we prescribe Dirichlet conditions. An exact solution is given by (cf. [5])

$$u = \frac{3}{4} - \frac{1}{4}\frac{1}{1+\exp((-4x+4y-t)/(32\cdot\varepsilon))} \tag{4.2a}$$

$$v = \frac{3}{4} + \frac{1}{4}\frac{1}{1+\exp((-4x+4y-t)/(32\cdot\varepsilon))}. \tag{4.2b}$$

The solution represents a wave front at $y = x + 0.25t$. The speed of propagation is $\sqrt{2}/8$ and is perpendicular to the wave front. We solve this problem at the time interval [0.0,3.0] and with $\varepsilon = 10^{-3}$.

For this example we will describe shortly how to write the user routines. The complete text of the user program is enclosed with the package.

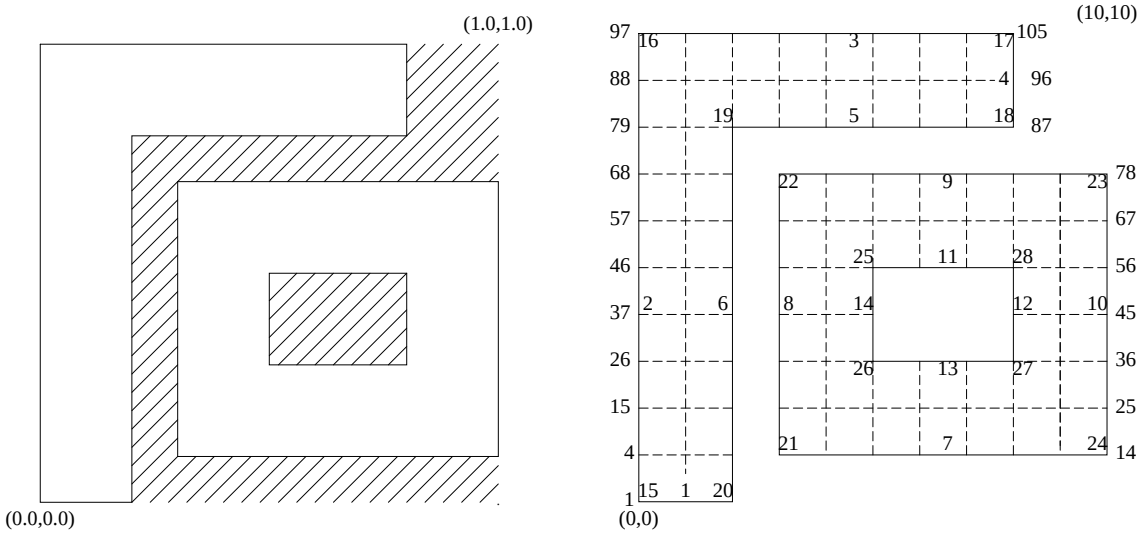

Figure 1: Example domain
Left the physical domain, right the base grid on the virtual rectangle.
Numbers at the left and the right are the node numbers of the grid points
Numbers inside the domain give the boundary or corner order as stored in the boundary structure

In the first call of `VLUGR2` the initial grid is formulated in the `INIDOM` routine, a refinement is enforced up to level 3 in the lower right corner of the physical domain, and the monitor routine is used to print the error after each time step and at each grid level. After $t = 1.0$ we will stop program 1, write all information to file and restart the computation with a different program reading the data from file. In that run we overload `DERIVF` with our own version which stores the exact partial derivatives $\partial \mathbf{F}/\partial \mathbf{U}_p$.

We enclose the domain by a virtual rectangle ((0.0,0.0),(1.0,1.0)) and make a virtual base grid of 11×11 grid points (cf. Fig. 1). For the first part of the time interval [0,1.0] the user program will contain

```
      MNTR = 0
      NPDE = 2
      T    = 0.0
      TOUT = 1.0
      DT   = 0.001
C Since domain is not a rectangle the grid parameters need not to be
C specified
      TOLS = 0.1
      TOLT = 0.05
      INFO(1) = 1
C MAXLEV
      INFO(2) = 5
C Domain not a rectangle
      INFO(3) = 1
C Linear system solver: GCRO + Diagonal scaling (no first order
C derivatives at the boundaries)
      INFO(4) = 13
C
      OPEN (UNIT=61,FILE='RunInfo')
```

```
C Write integration history to unit # 61
      INFO(5) = 61
C Write Newton info to unit # 61
      INFO(6) = 61
C Write GCRO info to unit # 61
      INFO(7) = 61
C DTMIN = 1E-7
      RINFO(1) = 1.0E-7
C DTMAX = 1.0
      RINFO(2) = 1.0
C UMAX = 1.0
      RINFO(3) = 1.0
      RINFO(4) = 1.0
C SPCWGT = 1.0
      RINFO(5) = 1.0
      RINFO(6) = 1.0
C TIMWGT = 1.0
      RINFO(7) = 1.0
      RINFO(8) = 1.0
C
C Call main routine
      CALL  VLUGR2 (NPDE, T, TOUT, DT, XL, YL, XR, YU, DX, DY,
     +   TOLS, TOLT, INFO, RINFO, RWK, LENRWK, IWK, LENIWK, LWK, LENLWK,
     +   MNTR)
```

Since we want to restart the computation we write an unformatted file with all the necessary information

```
      OPEN(UNIT=LUNDMP,FILE='DUMP',FORM='UNFORMATTED')
      CALL DUMP (LUNDMP, RWK, IWK)
      CLOSE(LUNDMP)
```

Next the PDE defining routines

```
      SUBROUTINE PDEIV
         . . .
      DO 10 I = 1, NPTS
         U(I,1) = 0.75 - 0.25/(1+EXP((-4*X(I)+4*Y(I)-T)/(32*EPS)))
         U(I,2) = 0.75 + 0.25/(1+EXP((-4*X(I)+4*Y(I)-T)/(32*EPS)))
   10 CONTINUE

      SUBROUTINE PDEF
         . . .
      DO 10 I = 2, NPTS-1
         RES(I,1) = UT(I,1) -
     +      (-U(I,1)*UX(I,1) - U(I,2)*UY(I,1) + EPS*(UXX(I,1)+UYY(I,1)))
         RES(I,2) = UT(I,2) -
     +      (-U(I,1)*UX(I,2) - U(I,2)*UY(I,2) + EPS*(UXX(I,2)+UYY(I,2)))
   10 CONTINUE

      SUBROUTINE PDEBC
         . . .
      NBNDS = LLBND(0)
```

```
      DO 10 K = LLBND(1), LLBND(NBNDS+1)-1
         I = LBND(K)
         RES(I,1) = U(I,1) -
     +           (0.75 - 0.25/(1+EXP((-4*X(I)+4*Y(I)-T)/(32*EPS))))
         RES(I,2) = U(I,2) -
     +           (0.75 + 0.25/(1+EXP((-4*X(I)+4*Y(I)-T)/(32*EPS))))
   10 CONTINUE
```

To define the initial grid in INIDOM one should store

```
XL = 0.0
YL = 0.0
XR = 1.0
YU = 1.0
DX = 0.1
DY = 0.1

LROW(0:12)  = (11, 1, 4, 15, 26, 37, 46, 57, 68, 79, 88, 97, 106)
IROW(1:11)  = (0, 1, 2, 3, 4, 5, 6, 7, 8, 9, 10)
ICOL(1:105) = (0, 1, 2,
               0, 1, 2, 3, 4, 5, 6, 7, 8, 9, 10,
               0, 1, 2, 3, 4, 5, 6, 7, 8, 9, 10,
               0, 1, 2, 3, 4, 5, 6, 7, 8, 9, 10,
               0, 1, 2, 3, 4, 5, 8, 9, 10,
               0, 1, 2, 3, 4, 5, 6, 7, 8, 9, 10,
               0, 1, 2, 3, 4, 5, 6, 7, 8, 9, 10,
               0, 1, 2, 3, 4, 5, 6, 7, 8, 9, 10,
               0, 1, 2, 3, 4, 5, 6, 7, 8,
               0, 1, 2, 3, 4, 5, 6, 7, 8,
               0, 1, 2, 3, 4, 5, 6, 7, 8)
```

For the boundaries, when numbered as in Fig. 1 the following should be stored in `LLBND`, `ILBND`, and `LBND`

```
LLBND(0:29) = ( 28,
                 1,  2, 11, 18, 19, 24, 31, 37, 42, 48, 53, 55, 56, 58,
                59, 60, 61, 62, 63, 64, 65, 66, 67, 68, 69, 70, 71, 72, 73)
ILBND(1:28) = (  1,  2,  3,  4,  1,  4,
                 1,  2,  3,  4,
                 1,  2,  3,  4,
                12, 23, 34, 41, 14, 41,
                12, 23, 34, 41,
                14, 43, 32, 21)
LBND(1: 72) = (  2,
                 4, 15, 26, 37, 46, 57, 68, 79, 88,
                98, 99,100,101,102,103,104,
                96,
                86, 85, 84, 83, 82,
                70, 59, 48, 39, 28, 17, 6,
                 8,  9, 10, 11, 12, 13,
                18, 29, 40, 49, 60,
                72, 73, 74, 75, 76, 77,
                67, 56, 45, 36, 25,
```

```
23  3  3  3  3  3  3  3 34 XX XX
 2 .. .. .. .. .. .. ..  4 XX XX
 2 .. 14  1  1  1  1  1 41 XX XX
 2 ..  4 23  3  3  3  3  3  3 34
 2 ..  4  2 .. .. .. .. .. ..  4
 2 ..  4  2 .. 14  1  1 21 ..  4
 2 ..  4  2 ..  4 XX XX  2 ..  4
 2 ..  4  2 .. 43  3  3 32 ..  4
 2 ..  4  2 .. .. .. .. .. ..  4
 2 ..  4 12  1  1  1  1  1  1 41
12  1 41 XX XX XX XX XX XX XX XX
```

Figure 2: Print out by the subroutine PRDOM of the example domain

```
  52, 53,
  43,
  33, 32
  42,
   1, 97, 105, 87, 81, 3, 7, 14, 78, 71, 51, 31, 34, 54)
```

To check if we defined the domain correct we print it out with

```
      INTEGER IDOM((NX+1)*(NY+1))
C
      LLBND(30) = LLBND(29)
      CALL PRDOM (LROW, IROW, ICOL, LLBND, ILBND, LBND,
     +   IDOM, NX, NY)
```

which prints internal points of the domain as .., external points as XX and for physical boundary points their ILBND value. The results are shown in Fig. 2.

To restart the computation we have to read the information from file and call VLUGR2 with MNTR = 1. In this run we use the default parameters. Note that the old values for T, DT, XL, YL, XR, YU, DX, and DY will be taken.

```
C Continuation call of VLUGR2
      TOUT = 3.0
      TOLS = 0.1
      TOLT = 0.05
      INFO(1) = 0
      MNTR = 1
C
      OPEN(UNIT=LUNDMP,FILE='DUMP',FORM='UNFORMATTED')
      CALL RDDUMP (LUNDMP, RWK, LENRWK, IWK, LENIWK)
      CLOSE(LUNDMP)
C
C call main routine
      CALL  VLUGR2 (NPDE, T, TOUT, DT, XL, YL, XR, YU, DX, DY,
     +   TOLS, TOLT, INFO, RINFO, RWK, LENRWK, IWK, LENIWK, LWK, LENLWK,
```

```
     +   MNTR)
```

For this run we want to use the exact partial derivatives $\partial \mathbf{F}/\partial \mathbf{U}_p$ and therefore we have overloaded DERIVF with our own subroutine of which contents we give a survey below

```
      SUBROUTINE DERIVF
         . . .
C A0: coefficient of U_n+1 in time derivative
C
Ccc Loop over the components of the (derivatives of) U
      IC = 1
C
C dF(U,Ut)/dU_ic
         DO 20 IPT = 1, NPTS
            FU(IPT,1,IC) = A0 - (-UX(IPT,1))
            FU(IPT,2,IC) = - (-UX(IPT,2))
   20    CONTINUE
C
C dF(Ux)/dUx_ic
         DO 40 IPT = 1, NPTS
            FUX(IPT,1,IC) = - (-U(IPT,1))
            FUX(IPT,2,IC) = 0.0
   40    CONTINUE

         . . .

      IC = 2
C
C dF(U,Ut)/dU_ic
         DO 120 IPT = 1, NPTS
            FU(IPT,1,IC) = - (-UY(IPT,1))
            FU(IPT,2,IC) = A0 - (-UY(IPT,2))
  120    CONTINUE

         . . .
C
C dF(Uyy)/dUyy_ic
         DO 180 IPT = 1, NPTS
            FUYY(IPT,1,IC) = 0.0
            FUYY(IPT,2,IC) = - (EPS)
  180    CONTINUE

C
C Correct boundaries (incl. the internal); all Dirichlet so FUp = 0.0
      NBNDS = LLBND(0)
      DO 100 LB = LLBND(1), LLBND(NBNDS+2)-1
         IPT = LBND(LB)
         FU(IPT,1,1) = 1.0
         FU(IPT,1,2) = 0.0
         FU(IPT,2,1) = 0.0
         FU(IPT,2,2) = 1.0
         FUX(IPT,1,1) = 0.0
```

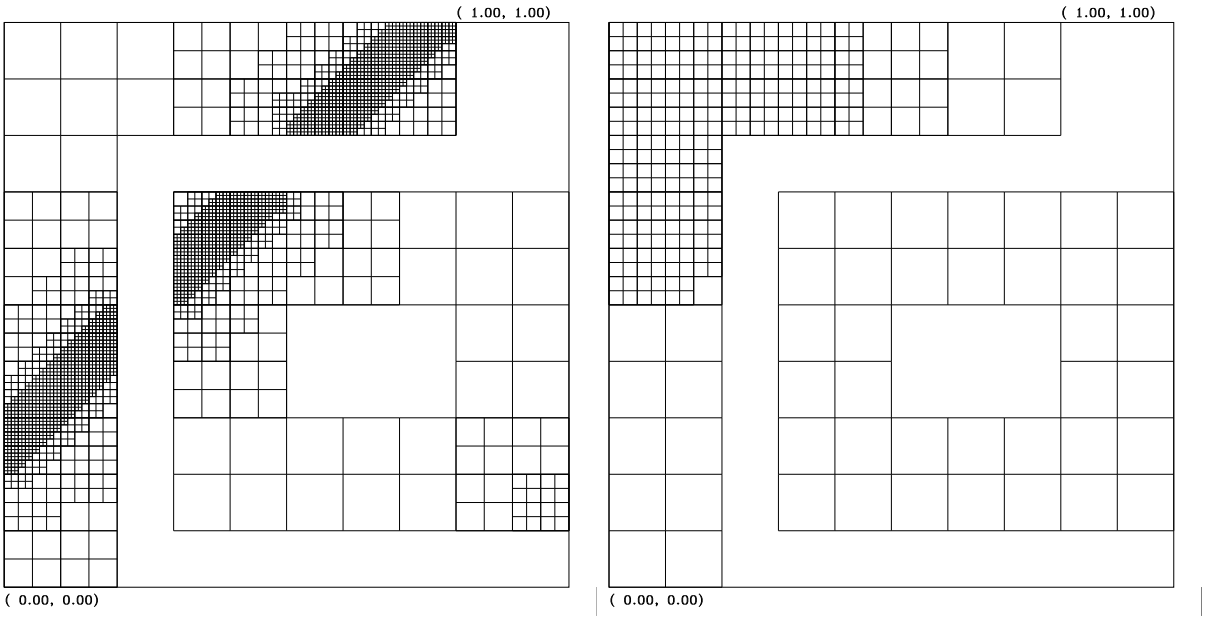

Figure 3: Grids for the example problem at $t = 1.0$ and at $t = 3.0$.

```
      . . .

      FUYY(IPT,2,2) = 0.0
100 CONTINUE
```

In Fig. 3 the generated grids after the final times of the first and the second program are shown. Recall that in the first run refinement up to order 3 is forced at the lower-right corner of the physical domain. The corresponding accuracy is, measured in the maximum norm, 0.01 at $t = 1.0$ and 0.08 at $t = 3.0$. Note that in the second run the number of grid levels is restricted to 3 which affects of course the accuracy.

5. Numerical experiments

In this section we discuss the test results obtained with `VLUGR2` for the groundwater-flow problems that were also used as examples in [14, 1].

5.1 Problem description: the 2D fluid-flow / salt-transport problem

In [14, 1] we consider a model for a non-isothermal, single-phase, two-component saturated flow problem which consists of 3 PDEs basic to groundwater flow: the continuity equation, the transport equation and the temperature equation. For the background of these equations we refer to [14]. We here present the model in non-conservative form. As independent variables we have the pressure p, the salt mass fraction ω, and the temperature T. The continuity equation for the fluid, the salt transport equation, and the temperature equation are given by

$$n\rho(\beta\frac{\partial p}{\partial t} + \gamma\frac{\partial \omega}{\partial t} + \alpha\frac{\partial T}{\partial t}) + \nabla\cdot(\rho\mathbf{q}) = 0, \tag{5.1a}$$

$$n\rho\frac{\partial \omega}{\partial t} + \rho\mathbf{q}\cdot\nabla\omega + \nabla\cdot(\rho\mathbf{J}^{\omega}) = 0, \tag{5.1b}$$

$$c^m \rho^m \frac{\partial T}{\partial t} + \rho c \mathbf{q} \cdot \nabla T + \nabla \cdot (\mathbf{J}^T) = 0, \tag{5.1c}$$

where n is the porosity parameter of the porous medium, β a compressibility coefficient, γ a salt coefficient, α a temperature coefficient, $c^m \rho^m$ a density expression satisfying $c^m \rho^m = nc\rho + (1-n)c^s \rho^s$, and c the specific heat capacity of the porous medium. Darcy's law gives the equation for the fluid velocity $\mathbf{q} = (q_1, q_2)^T$

$$\mathbf{q} = -\frac{k}{\mu}(\nabla p - \rho \mathbf{g}), \tag{5.2}$$

with $\mathbf{g}$ the acceleration-of-gravity vector and k the permeability coefficient of the porous medium. The density ρ and the viscosity μ obey the state equations

$$\rho = \rho_0 \exp[\alpha(T - T_0) + \beta(p - p_0) + \gamma\omega], \tag{5.3}$$

$$\mu = \mu_0(T) \cdot m(\omega),\ m(\omega) = 1 + 1.85\omega - 4.0\omega^2, \tag{5.4}$$

where ρ_0 is the reference density of fresh water, p_0 a reference pressure, T_0 a reference temperature, and $\mu_0(T)$ a possibly temperature-dependent reference viscosity. The equation for the salt-dispersion flux vector is given by Fick's law

$$\mathbf{J}^\omega = -n\mathbf{D}\nabla\omega, \tag{5.5}$$

with the dispersion tensor $\mathbf{D}$ for the solute salt defined as

$$n\mathbf{D} = (nD_{mol} + \alpha_T|\mathbf{q}|)I + \frac{\alpha_L - \alpha_T}{|\mathbf{q}|}\mathbf{q}\mathbf{q}^T,\ |\mathbf{q}| = \sqrt{\mathbf{q}^T\mathbf{q}}. \tag{5.6}$$

The coefficients D_{mol}, α_T and α_L correspond, respectively, with the molecular diffusion and the transversal and longitudinal dispersion. Finally, the heat-flux vector $\mathbf{J}^T$ is given by

$$\mathbf{J}^T = -\mathbf{H}\nabla T, \tag{5.7}$$

where $\mathbf{H}$, the heat conductivity tensor of the porous medium, is defined as

$$\mathbf{H} = (\kappa + \lambda_T|\mathbf{q}|)I + \frac{\lambda_L - \lambda_T}{|\mathbf{q}|}\mathbf{q}\mathbf{q}^T. \tag{5.8}$$

The parameter κ is the coefficient of heat conductivity and λ_T and λ_L are, respectively, the transversal and longitudinal heat conductivity coefficients.

Our examples are connected with Intraval test case 13 [7]. This laboratory experiment deals with the displacement of fresh water by brine in a thin vertical column filled with a porous medium. Salt water of a high concentration is injected through gates at the bottom of the column giving rise to a fresh-salt water front moving in all directions into the column.

5.1.1 Data for Problem I. In [7] the experiment was carried out under isothermal conditions. We assume non-isothermal conditions and suppose that warm brine is injected. Because the column is very thin, the flow can be considered as being two-dimensional. In our numerical experiment it is supposed that two gates are used for salt water injection so that initially two disjunct salt / fresh water fronts exist which later interact and merge into one front. Due to dispersion the fronts smooth out with time in all directions. For t sufficiently large the fronts disappear completely which means that the whole medium is filled with the high-salt-concentration fluid.

In Problem I the model is considered on the time-space domain $[0, t_{end}] \times \Omega$ where the flow domain Ω representing the vertical column is the unit square $\Omega = \{(x, y) | 0 < x, y < 1\}$. Since Ω represents a vertical cross section, the independent variable y stands for a vertical variable with unit vector pointing upward. Hence the acceleration of gravity vector takes the form $\mathbf{g} = (0, -g)^T$, where g is the gravity constant. The initial values at $t = 0$ at $\Omega \cup \partial\Omega$ are taken as

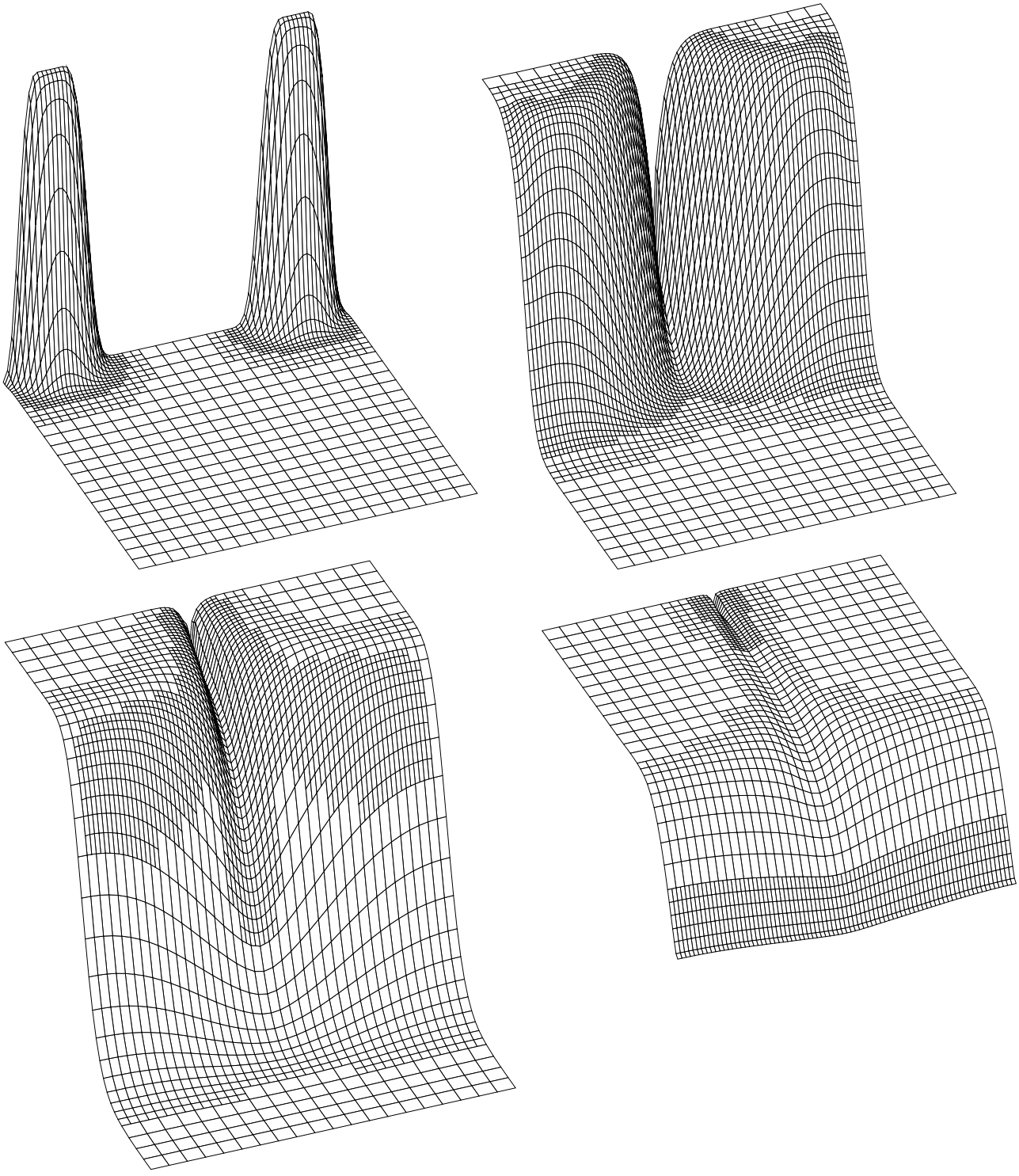

Figure 4: Distribution of salt concentration at $t = 500, 5000, 10000$ and 20000 with the corresponding grid configuration.

n	0.4	λ_T	0.001	β	$4.45\,10^{-10}$
k	10^{-10}	λ_L	0.01	γ	$\ln(1.2)$
g	9.81	c^s	840	μ_0	10^{-3}
D_{mol}	0.0	ρ^s	2500	ω_0	0.25
α_T	0.002	ρ_0	1000	q_c	10^{-4}
α_L	0.01	T_0	290	T_c	292
c	4182	p_0	10^5	t_{end}	$2\,10^4$
κ	4.0	α	$-3\,10^{-4}$		

Table 1: Data for Problem I.

$$p(x,y,0) = p_0 + (1-y)\rho_0 g, \quad \omega(x,y,0) = 0, \quad \text{and} \quad T(x,y,0) = T_0, \tag{5.9}$$

which correspond, respectively, to hydrostatic pressure, fresh water and a non-heated medium. For $0 < t \le t_{end}$ the following boundary conditions are imposed

$$\begin{array}{lll}
x = 0,1, & 0 \le y \le 1: & q_1 = 0,\ \omega_x = 0,\ T_x = 0, \\
y = 1, & 0 < x < 1: & p = p_0,\ \omega_y = 0,\ T_y = 0, \\
y = 0, & \frac{1}{11} \le x \le \frac{2}{11},\ \frac{9}{11} \le x \le \frac{10}{11}: & q_2 = q_c,\ \omega = \omega_0,\ T = T_c, \\
y = 0, & 0 < x < \frac{1}{11}, & \\
 & \frac{2}{11} < x < \frac{9}{11},\ \frac{10}{11} < x < 1: & q_2 = 0,\ \omega_y = 0,\ T_y = 0.
\end{array} \tag{5.10}$$

The third line is connected with the two gates where the warm brine is injected with a prescribed velocity and concentration. The other conditions are self-evident. All remaining problem data are contained in Table 1.

We have run this example using the following set of numerical parameters

$$\Delta t_0 = 0.1 \quad \text{and} \quad \Delta x = 0.05, \quad \Delta y = 0.05,$$

$$\texttt{TOLS} = 0.1 \quad \text{and} \quad \texttt{TOLT} = 0.1,$$

$$\texttt{UMAX} = (1.1\text{E}+5, 0.25, 292).$$

For all other parameters we used the default choice. Since Δx and Δy are the cell widths of the coarse base grid and $\texttt{MAXLEV} = 3$ this results in a finest grid size allowed of 1/80. Although this is small enough to avoid wiggles, at most time intervals the refinement is restricted by `MAXLEV` and not by `TOLS`.

In Fig. 4 we show the distribution of salt concentration at various time levels with the corresponding grid configuration. The temperature distribution shows a comparable behavior, but less steep and slower in time. The results for all solvers are alike.

5.1.2 Data for Problem II. In the second example we consider the case of total impermeability for part of the flow domain, viz., the region $\{(x,y) | 0 \le x \le 0.5,\ 0.4 \le y \le 0.6\}$. We also consider the flow now to be isothermal and incompressible ($\alpha = \beta = 0$).

The boundary conditions for the impermeability region are

$$\begin{array}{lll}
0 \le x \le 0.5, & y = 0.4, 0.6: & p_y = -\rho g, \quad \omega_y = 0, \\
x = 0.5 & 0.4 < y < 0.6: & p_x = 0, \quad \omega_x = 0.
\end{array} \tag{5.11}$$

We have closed the right gate so that salt water is injected only through the left gate. Hence we deal with a single salt / fresh water front which first collides with the region of impermeability and then must flow around it. For this problem we run until steady state is reached ($\omega \equiv \omega_0$), i.e., $t_{end} = 10^5$. All other parameters, if required, are chosen as in Problem I.

The distribution of the salt concentration at various time levels with the corresponding grid configuration is shown in Fig. 5.

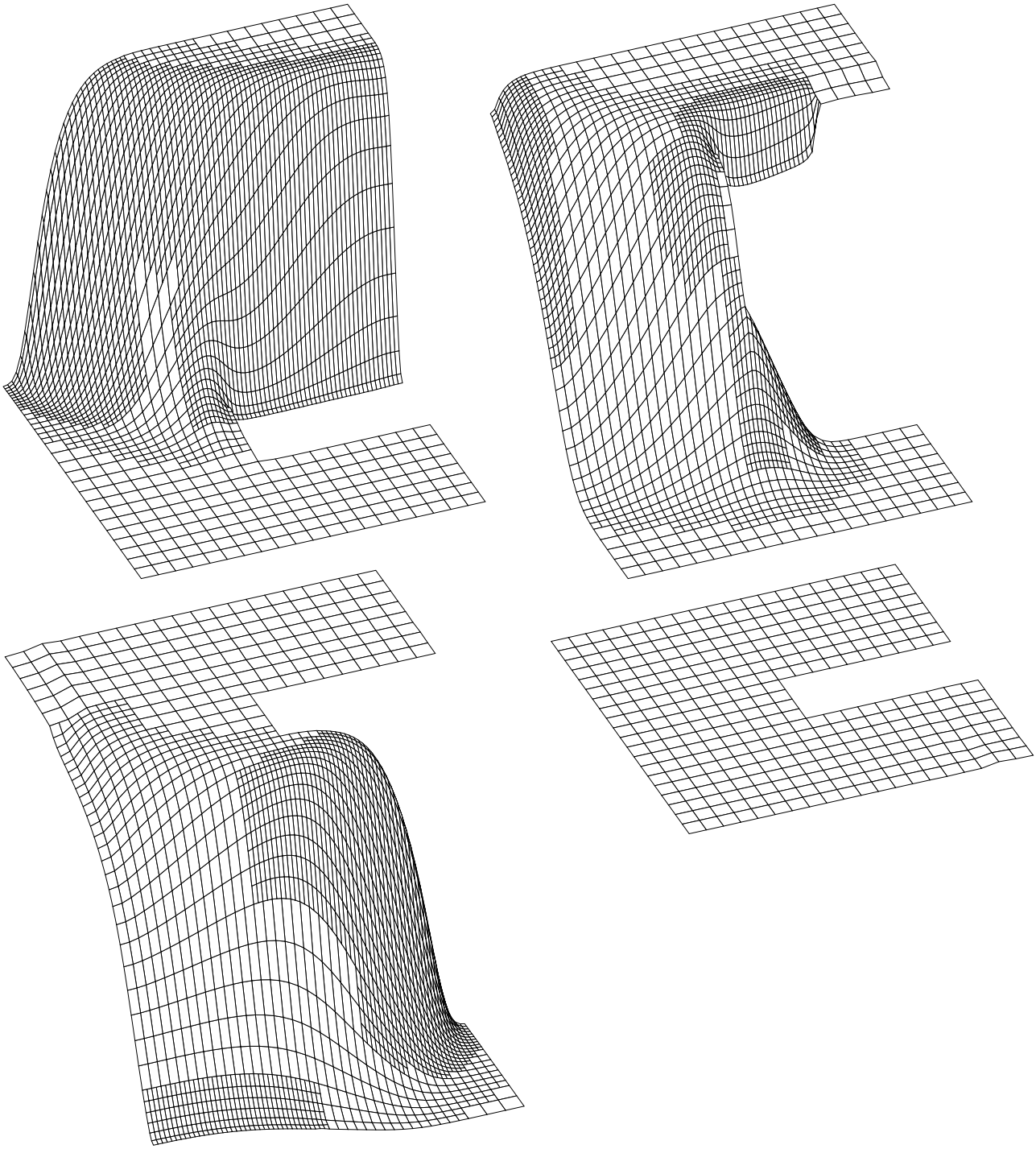

Figure 5: Distribution of salt concentration at $t = 10000, 20000, 30000$ and 100000 with the corresponding grid configuration.

Solver preconditioner		BiCGStab ILU	GCRO diagonal	GCRO block-diag	matrix-free GCRO block-diag
# time steps		197	197	197	207
# Newton it./level	1	396	396	396	430
	2	396	396	396	440
	3	396	396	396	472
# Lin. sys. it. per					
Newton it., level	1, 1	1045	8962	8894	9960
	1, 2	763	14691	14558	15811
	1, 3	746	15978	15372	20239
	2, 1	278	7005	6792	8304
	2, 2	429	7135	7066	12857
	2, 3	467	6978	7025	17117
	3, 1		66	66	273
	3, 2				596
	3, 3				3721
	4, 1				84
	4, 2				389
	4, 3				736
	5, 2				82

Table 2: Integration history for Problem I.

Solver preconditioner		BiCGStab ILU	GCRO diagonal	GCRO block-diag	matrix-free GCRO block-diag
# time steps		306	305	305	334
# Newton it./level	1	614	612	612	718
	2	604	602	602	709
	3	548	544	544	667
# Lin. sys. it. per					
Newton it., level	1, 1	1831	15984	15759	18058
	1, 2	1239	24433	24042	27330
	1, 3	1215	24208	24243	29995
	2, 1	782	10914	10198	14686
	2, 2	899	10553	10083	21131
	2, 3	823	11027	10218	24439
	3, 1				1027
	3, 2				1702
	3, 3				4808
	4, 1				309
	4, 2				496
	4, 3				1032
	5, 1				189
	5, 2				147
	5, 3				163
	6, 3				120

Table 3: Integration history for Problem II.

5.2 Integration history

In Tables 2 and 3 we give the integration history for Problem I and II, respectively. The number of linear system iterations given under GCRO is the sum of the outer-loop iterations (the GCR process) and the inner-loop iterations (GMRES 'preconditioner'). For both problems the solvers using the Jacobian explicitly are very robust. Note that without preconditioning GCRO, with the default values `MAXLR` = 5 and `MAXL` = 20, most probably would outperform BiCGStab, so the ILU preconditioner does a good job. The diagonal and the block-diagonal preconditioner both take into account the first-order derivatives at the boundaries. The difference in performance between the two is minor, the number of iterations decreases only slightly. For the matrix-free version the difference between these two preconditioners is much clearer. Using block-diagonal preconditioning the matrix-free solver only occasionally suffers from time step rejections due to Newton failures. With diagonal scaling this number is much higher.

5.3 Global performance

		BiCGStab ILU		GCRO diagonal		GCRO block-diag		matrix-free GCRO block-diag	
		CP sec	Mflop	CP sec	Mflop	CP sec	Mflop	CP sec	Mflop
Problem I	scalar	368	16	820	28				
	vector	74	78	138	162	143	158	275	193
Problem II	scalar	220	16	485	31				
	vector	50	71	100	149	101	147	242	173

Table 4: Global performance.

Our performance evaluation was done on a Cray Y-MP with the CF77 compiling system. Scalar results were obtained using `cf77 -Wf"-o novector"`, and vector results with `cf77 -Zv -Wf"-o aggress"`. The timings were done on 1 processor with a clock cycle time of 6ns. This gives a theoretical peak performance on 1 processor of 167 Mflops and 333 when chaining an add and a multiply. Since during one cycle time 1 store and 2 loads can be performed, indirect addressing of (one of) the vector operands of a triad will reduce the performance at least with a factor of 2, bank conflicts left out of consideration. When more vectors are indirectly addressed the (current) impossibility on the Y-MP to chain more than one gathered/scattered load/store would reduce the performance to a much larger degree. To measure the Megaflop rate and the CPU time of a routine we used the Cray utility Perftrace[6], that gives the hardware performance by program unit.

We first give a global idea of the performance of the different solvers. In Table 4 the CPU time and the Mflop rate is shown for both example problems. It is clear that although the (matrix-free) GCRO solver reaches an almost optimal vector speed, considering that we use indirect addressing, the CPU time is (much) larger than when we use BiCGStab + ILU. This is due to the fact that the number of iterations needed is so much higher.

5.4 Vector results

In this section we will compare the vector performance of the solvers.

Tables 5 and 6 show the vector performance of the five routines that use the most CPU time (accumulated). One can see that the PDE definition on the internal domain (`PDEF`) vectorizes nicely, as expected, since no exceptions have to be made. The definition of the boundary conditions (`PDEBC`) run at a lower Mflop rate of about 65, but this routine takes only 1% of the total CPU time. All in all it appears that, with the exception of the preconditioning, `VLUGR2` + BiCGStab is an efficiently vectorized code. The routines needed for the irregular grid structure and refinement take together less than 5% of the CPU time (in vectorized mode). So the overhead for the grid refinement is negligible

BiCGStab+ILU					GCRO+Diagonal				
	# calls	Avg time	ACM %	Mflop		# calls	Avg time	ACM %	Mflop
ILU backs	8688	3.2E-3	37.5	39	MATVEC	60973	1.1E-3	47.9	137
ILU dec	591	2.6E-2	58.5	23	GMRES	3502	1.4E-2	82.8	209
PDEF	11826	1.1E-3	75.4	213	PDEF	11826	1.1E-3	91.9	212
MATVEC	7500	9.9E-4	85.4	138	INJON	1174	1.5E-3	93.2	0
INJON	1174	1.5E-3	87.7	0	GCR	1188	1.4E-3	94.4	108
GCRO+Block-diag					matrix-free GCRO+Block-diag				
	# calls	Avg time	ACM %	Mflop		# calls	Avg time	ACM %	Mflop
MATVEC	59931	1.1E-3	44.9	138	PDEF	101494	1.3E-3	48.7	214
GMRES	3485	1.3E-2	77.2	209	GMRES	4823	1.6E-2	76.4	217
PDEF	11826	1.1E-3	86.0	212	DERIVS	91571	3.1E-4	86.7	158
Bl. backs	61119	1.3E-4	91.3	109	Bl. backs	1571	1.4E-4	91.3	111
INJON	1174	1.5E-3	92.6	0	MATVEC	90169	7.6E-5	93.7	160

Table 5: Vector performance of top 5 routines for Problem I.
ACM %: Accumulated percentage of CPU-time spent

BiCGStab+ILU					GCRO+Diagonal				
	# calls	Avg time	ACM %	Mflop		# calls	Avg time	ACM %	Mflop
ILU backs	15398	1.3E-3	40.8	33	GMRES	5421	8.4E-3	45.5	177
PDEF	12326	6.3E-4	56.4	209	MATVEC	97260	3.7E-4	81.7	133
ILU dec	880	6.6E-3	68.2	21	PDEF	12270	6.2E-4	89.3	210
MATVEC	13632	3.6E-4	78.1	133	GCR	1758	1.1E-3	91.2	73
INJON	1710	1.0E-3	81.6	0	INJON	1701	1.0E-3	93.0	0
GCRO+Block-diag					matrix-free GCRO+Block-diag				
	# calls	Avg time	ACM %	Mflop		# calls	Avg time	ACM %	Mflop
GMRES	5380	8.1E-3	42.8	178	PDEF	158253	7.2E-4	46.9	209
MATVEC	94684	3.7E-4	77.2	135	GMRES	7680	9.2E-3	76.1	178
PDEF	12270	6.2E-4	84.7	211	DERIVS	147830	1.9E-4	87.4	125
Bl. backs	96442	4.1E-5	88.6	101	Bl. backs	7830	4.3E-5	90.0	100
GCR	1758	1.1E-3	90.4	69	MATVEC	145632	4.1E-5	92.5	138

Table 6: Vector performance of top 5 routines for Problem II.
ACM %: Accumulated percentage of CPU-time spent

as long as we need to solve our problems with an implicit time integrator.

6. Summary

In this paper we described `VLUGR2`, a vectorizable Method of Lines solver based on a Local Uniform Grid Refinement method for systems of time-dependent PDEs in two space dimensions. Our code offers three different solvers for the nonlinear systems. In the first two the Jacobian of the Newton process is approximated and stored. The linear solvers are BiCGStab[17] combined with standard ILU preconditioning and GCRO[8] with (block) diagonal scaling. The third nonlinear solver is a matrix-free Newton process with as linear solver GCRO. An advantage of a matrix-free solver is that tailor-made space-discretization schemes, resulting in other couplings than the here used 9-point stencil, can be more easily implemented. For a large number of PDE components its memory use can also be profitable. However it is less robust and generally uses more CPU time even though the vector performance of this solver is very good.

We discussed the performance of `VLUGR2` for two groundwater-flow problems. The LUGR method proves to be robust and efficient with respect to the location of the refined grids. The nonlinear solvers that make explicit use of the Jacobian both are reliable. BiCGStab with as preconditioner the vectorized implementation of the ILU decomposition of the Jacobian is for these problems computationally the most efficient. Since in two dimensions memory requirements are often not the bottleneck, we strongly advocate the use of this solver.

References

1. J.G. Blom and J.G. Verwer. VLUGR2: A vectorized local uniform grid refinement code for PDEs in 2D. Report NM-R9306, CWI, Amsterdam, 1993.
2. J.G. Blom and J.G. Verwer. Vectorizing matrix operations arising from PDE discretization on 9-point stencils. *The Journal of Supercomputing*, 8:29–51, 1994.
3. J.G. Blom and J.G. Verwer. VLUGR3: A vectorizable adaptive grid solver for PDEs in 3D. I. Algorithmic aspects and applications. Report NM-R9404, CWI, Amsterdam, 1994.
4. J.G. Blom and J.G. Verwer. VLUGR3: A vectorizable adaptive grid solver for PDEs in 3D. II. Code description. Report NM-R9405, CWI, Amsterdam, 1994.
5. J.H.M. ten Thije Boonkkamp. *The Numerical Computation of Time-Dependent, Incompressible Fluid Flow*. PhD thesis, University of Amsterdam, the Netherlands, 1988.
6. Cray Research, Inc. *UNICOS Performance Utilities Reference Manual*, SR-2040 6.0 edition, 1991.
7. S.M. Hassanizadeh, A. Leijnse, W.J. de Vries, and R.A.M. Stapper. Experimental study of brine transport in porous media, Intraval test case 13. Report 725206003, National Institute of Public Health and Environmental Protection, Bilthoven, the Netherlands, 1990.
8. E. de Sturler and D.R. Fokkema. Nested Krylov methods and preserving the orthogonality. Preprint NR. 796, Department of Mathematics, University of Utrecht, the Netherlands, 1993.
9. R.A. Trompert. MOORKOP, an adaptive grid code for initial-boundary value problems in two space dimensions. Report NM-N9201, CWI, Amsterdam, 1992.
10. R.A. Trompert. *Local Uniform Grid Refinement for Time-Dependent Partial Differential Equations*. PhD thesis, University of Amsterdam, the Netherlands, 1994.
11. R.A. Trompert and J.G. Verwer. A static-regridding method for two-dimensional parabolic partial differential equations. *Appl. Numer. Math.*, 8:65–90, 1991.
12. R.A. Trompert and J.G. Verwer. Analysis of the implicit Euler local uniform grid refinement method. *SIAM J. Sci. Comput.*, 14:259–278, 1993.
13. R.A. Trompert and J.G. Verwer. Runge-Kutta methods and local uniform grid refinement. *Math. Comp.*, 60:591–616, 1993.

14. R.A. Trompert, J.G. Verwer, and J.G. Blom. Computing brine transport in porous media with an adaptive-grid method. *Int. J. Numer. Meth. in Fluids*, 16:43–63, 1993.

15. J.G. Verwer and R.A. Trompert. An adaptive-grid finite-difference method for time-dependent partial differential equations. In D.F. Griffiths and G.A. Watson, editors, *Proc. 14-th Biennial Dundee Conference on Numerical Analysis*, pages 267–284. Pitman Research Notes in Mathematics Series 260, 1992.

16. J.G. Verwer and R.A. Trompert. Analysis of local uniform grid refinement. *Appl. Numer. Math.*, 13:251–270, 1993.

17. H.A. van der Vorst. BI-CGSTAB: A fast and smoothly converging variant of BI-CG for the solution of nonsymmetric linear systems. *SIAM J. Sci. Stat. Comput.*, 13(2):631–644, 1992.